New Cable-Driven Continuum Robot with Only One Actuator

New Cable-Driven Continuun Robot with Only One Actuator

Zhongning JIANG, Yuanxin LUO
School of Mechanical Engineering, Chongqing University
Chongqing, China
yxluo@cqu.edu.cn

Yan JIN
Dept. of Mechanical &Aerospace Engineering, Queen's University Belfast
Belfast, UK

***Abstract*—This paper presents a new cable-driven continuum robot by using the time-based control method with only actuator. The continuum robot consists of 3 sections, and each section has 2 DOFs. It is driven by a constant speed motor connected to a series of electromagnetic clutches. The clutches will be activated for providing the motion of the cables. A new time-based control method named 'Time Width Modulation' is proposed to control the continuum robot. Kinematics and workspace analyses are carried out. A prototype is built up and experimental results demonstrate the effectiveness of the proposed design and control method.**

Keywords—Continuum robot; cable-driven; time-based control method; time-sequence diagram

I. INTRODUCTION

The continuum robot has been a hot topic in research. As the require of working in confined environments, such as minimally invasive surgery and disaster rescue, many continuum robots have been invented during the last decades. Due to its high degree of freedom (DOF), the actuator has been one of key issue for continuum robot.

There are different kinds of actuators for continuum robot, such as pneumatic artificial muscle and shape memory alloy. For instant, Walker *et al* [1-2] designed a soft robotic manipulator, called OCTARM. It adopts McKibben air muscles as actuators and has a total of 12 DOFs. OCTARM can grasp things by wrapping tightly around it. Therefore, this kind of robotic manipulator has accurate grasping configurations and can move flexibly along the ideal path. It has great advantages in avoidance of obstacles and grasping heavy load. Simaan *et al* [3] developed a medical continuum robot arm that is used for throat surgery. This robot consists of two parts, including two joints and three NiTi alloy tubes as the actuators. The NiTi alloys are used to drive the joints so that the robot can bend. Since each of the joints of the robot has two degrees of freedom, it has a total of four degrees of freedom. FESTO Company [4] developed a Bionic Handling Assistant (BHA). This manipulator is made of polyamide and pneumatically actuated. It consists of three segments. The BHA can move stably and bear heavy loads. FESTO also presents a model for the simulation and experiment with BHA. Webster III *et al* [5] designed a miniature snakelike surgical robot, called Active Cannulas (AC). It consists of several telescoping pre-curved super-elastic tubes and use elastic energy stored in the backbone to create bending. Unlike the traditional structure, this robot can be very small and may be quite useful in the near future.

Due to the flexibility and low cost, cable-driven mechanisms have been used for developing continuum robot arms. Moreover, the actuators can be mounted far away from the end effector in a cable driven robot, which will be of great importance to minimize the size of the end effector. Therefore, many research took efforts on the type of continuum robot. For example, Camarillo *et al* [6] developed a cable-driven continuum robot, which has three joints and 6 DOFs, and each joint is driven by four cables that with 2 DOFs. It is of practical significance that the interior of the robot is a hollow tube structure so that it can carry a camera or any other instruments, allowing the robot to perform a wide variety of operations. Bukinghan *et al* [7] designed and manufactured snake-arm robots for remote handling operations in confined and hazardous spaces in OC Robotics. OC Robotics also developed well-known snake-like robots driven by cables for nuclear, aerospace and security. Gravagne *et al*[8] presented the Clemson Tentacle Manipulator (CTM) used highly elastic rod as its backbone and antagonistic cable pairs to deform its shape. This kind of structure is light in weight and can adopt numerous poses for a given actuator displacement. Choi *et al* [9] proposed a kind of continuum robot with a spring backbone and driven by cables. Under the support of springs, the robot can keep constant curvature while it is bending. Unlike other robots mentioned above, this robot can extend along the length direction. Li *et al* [10] designed and built a wire-driven serpentine robot arm. The robot has 2 DOFs, and its positioning error is less than 2%. The kinematics is also researched. Moreover, they built a robot arm with 6 DOFs [11]. And the experiments are carried out, which turns out that the robot has high positioning accuracy.

However, all the continuum robots mentioned above were driven by many actuators, and the number of actuators is equal to the number of DOFs. This will inevitably lead to a higher cost and complexity in controlling all these actuators simultaneously. To solve this problem, this paper presents a new continuum robot system of 6 DOFs driven by only one actuator. A simple time-based control method is proposed to control the continuum robot

II. Design And Modeling Of The Continuum Robot

The structure of the robot in this paper is bio-inspired, and use the same structure in [10]. As shown in Figure 1(a), the robot is connected by 12 segments connected via spherical joints. The robot can bend towards any direction in space, and the motion can be very flexible due to the spherical joint. There is a central hole in each segments. The prototype is made of ABS (Acrylonitrile Butadiene Styrene) by 3D printing. The parameters of each segment are shown in Table I.

As shown in Figure 1(b), there are 12 holes on each segment for the passing though of cables. The robot can be divided into three sections, and each section consists of 4 segments and driven by 2 sets of cables. As shown in Figure 1(b), P_{1x} (x = 1, 2, 3, 4) makes up a set of cables for driving one section. Each section can bend in two directions by the two sets of cables in 3D space. For example, P_{11} and P_{13} control the bending around the x direction; while P_{12} and P_{14} control the bending around the y direction. These two bending motions are all independent to each other.

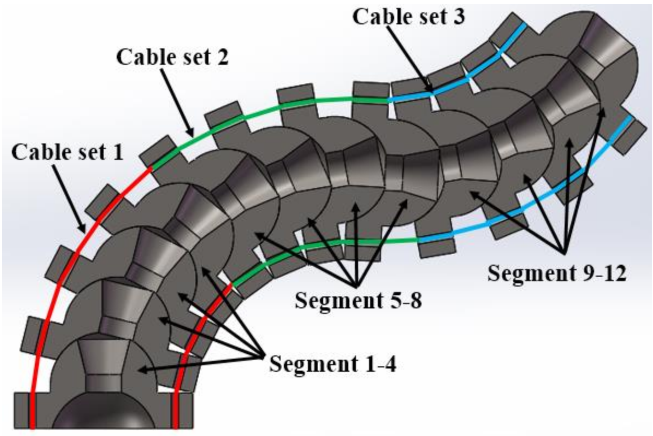

(a)

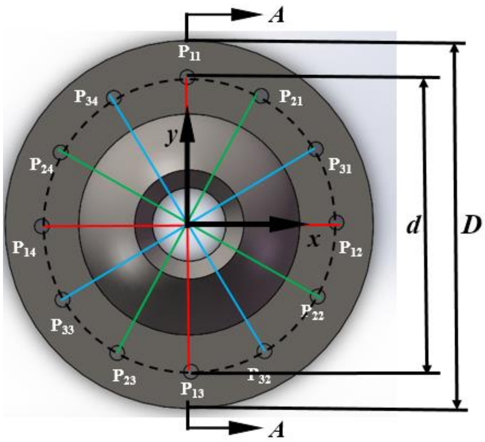

(b)

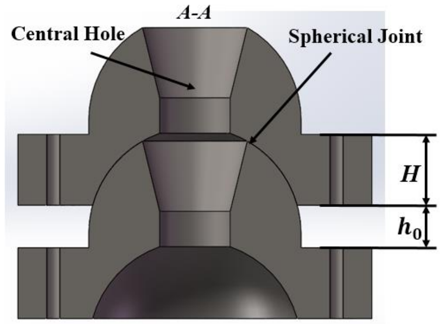

(c)

Fig.1 Illustration of the robot: a) CAD model, b) top view, and c) cross-section view for two segments

TABLE I. PARAMETERS OF THE SEGMENT

Parameters	***Values***
Outer Diameter(D)	50mm
Inner Diameter(D_1)	10mm
Diameter of the Circle of Pilot Hole(d)	40mm
Pilot Hole Diameter(d_1)	2mm
Segment Height(H)	10mm
Gap Distance(h_0)	6mm
Diameter of the Spherical Joint(D_1)	30mm
Maximum bending angle(θ_{max})	13.68°

A. *Kinematics Mapping of the Robot*

It is difficult to directly get the relationship between cables and the distal end position of the robot [12]. To describe the cable-driven mechanism, the forward/inverse kinematics are given in Figure 2. It presents the relations between actuator space to configuration space and task space. The actuator space stands for the cable length l, the configuration space stands for the robot bending angles θ or Φ, and the task space stands for the end effector's position and orientation.

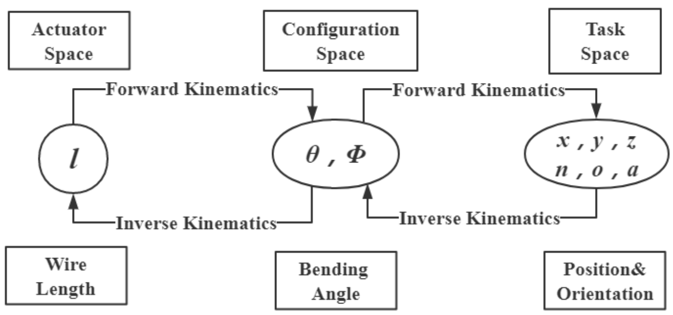

Fig.2 Kinematics mapping of the difference spaces

B. *Kinematics of the One Section*

1) Mapping between actuator space and configuration space

The forward kinematics of a single section between actuator space and configuration space can be obtained [11]:

$$\Phi = arctan\left(\frac{L_2 - L_4}{L_1 - L_3}\right) \quad (1)$$

$$\Theta = N \cdot \theta = 2N \cdot arcsin\left[\frac{\sqrt{(L_1 - L_3)^2 - (L_2 - L_4)^2}}{2N \cdot d}\right] \quad (2)$$

And the inverse kinematics is:

$$L_1 = L_0 + 2N\left[bsin\left(\frac{\theta}{2}\right) - h_0 sin^2\left(\frac{\theta}{4}\right)\right] \quad (3)$$

$$L_2 = L_0 + 2N\left[asin\left(\frac{\theta}{2}\right) - h_0 sin^2\left(\frac{\theta}{4}\right)\right] \quad (4)$$

$$L_3 = L_0 - 2N\left[bsin\left(\frac{\theta}{2}\right) + h_0 sin^2\left(\frac{\theta}{4}\right)\right] \quad (5)$$

$$L_4 = L_0 - 2N\left[asin\left(\frac{\theta}{2}\right) + h_0 sin^2\left(\frac{\theta}{4}\right)\right] \quad (6)$$

Where θ is the bending angle of each segment, Θ is the total bending angle of a section, Φ is the bending direction angle of a section, $L_1 \sim L_4$ are the cable lengths of the cables in each section, $a = (d/2)sin(\Phi)$ and $b = (d/2)cos(\Phi)$.

Note that the maximum bending angle, θ_{max}, of the joint is constrained by the segment parameters, D and h_0. The relationship between θ_{max} and the segment parameters is as follows:

$$\theta_{max} = 2arctan\left(\frac{h_0}{D}\right) \quad (7)$$

2) Mapping between configuration space and task space

As shown in Figure 3, the bold solid lines represent the central axes of the segment. For one section, the angel in between two consecutive segments is θ. When the robot is bent, the axes of segments can be considered as a polygon with exterior angle of θ, and the side length is $H + h_0$. Obviously, the radius is:

$$R = \frac{H + h_0}{2sin(\theta/2)} \quad (8)$$

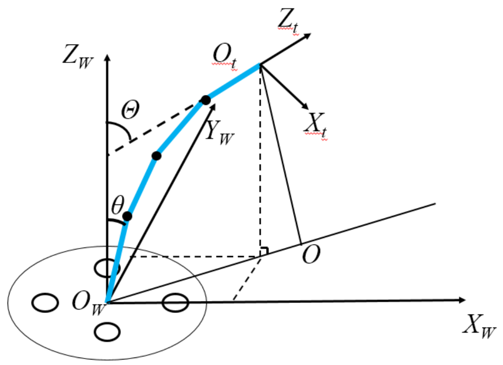

Fig.3 The robot bending sketch

According to the geometry relationship given in the Figure 3, the position of end effector can be described as:

$$\begin{cases} x = R(1 - cosN\theta)cos\Phi \\ y = R(1 - cosN\theta)sin\Phi \\ z = RsinN\theta \end{cases} \quad (9)$$

The forward kinematics mapping between configuration space and task space can be obtained by equations (8) and (9). Its inverse kinematics can be derived as:

$$\Theta = N \cdot \theta = 2arctan\left(\frac{\sqrt{x^2 + y^2}}{z}\right) \quad (10)$$

$$\Phi = arctan\left(\frac{y}{x}\right) \quad (11)$$

C. *Kinematics of the Multi-Section Robot*

The kinematics of the multi-section robot can be divided into forward kinematics and inverse kinematics. The forward kinematics is given by a 4 by 4 matrix:

$$T_3^W = T_1^W \cdot T_2^1 \cdot T_3^2 \quad (12)$$

Where

$$T_i^{i-1} = T = \begin{bmatrix} C\Theta_i C^2\Phi_i + S^2\Phi_i & (C\Theta_i - 1)C\Phi_i S\Phi_i & S\Theta_i C\Phi_i & dx \\ (C\Theta_i - 1)C\Phi_i S\Phi & C\Theta_i S^2\Phi_i + C^2\Phi_i & S\Theta_i S\Phi_i & dy \\ -S\Theta_i C\Phi_i & -S\Theta_i S\Phi_i & C\Theta_i & dz \\ 0 & 0 & 0 & 1 \end{bmatrix} \quad (13)$$

A 4×4 transformation matrix can be obtained by solving equation (12). In this matrix, the first three columns represent the orientation information of the end effector, and the forth column is its position information.

As there is no unique solution for the inverse kinematics due to the DOFs of the robot. Li *et al* [11] proposed a uniform bending scheme to make sure that it has the unique solution. In this scheme, the bending angle Θ_i is set to be same. And the bending motions are assumed to take place in the same plane. Hence, one can get $\Theta_1 = \Theta_2 = \cdots = \Theta_M$, and $\Phi_1 = \Phi_2 = \cdots = \Phi_M$, Substituting the two conditions into equations (12) and (13), it is easy to get the inverse solution as follows:

$$\Phi = arctan\left(\frac{y}{x}\right) \quad (14)$$

$$R = \frac{x^2 + y^2 + z^2}{2\sqrt{x^2 + y^2}} \quad (15)$$

$$\Theta = \frac{1}{M} arcsin\left(\frac{z}{R}\right) \quad (16)$$

D. *Workspace*

By setting Θ and Φ, we can get the simulation workspace of multi-section robot, as shown in Figure 4. Obviously, the reachable distances from the origin are about 150mm and 190mm in X-Y and Z direction, respectively.

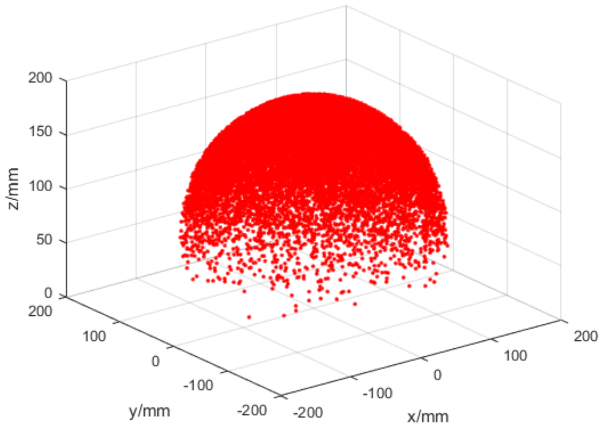

(a)

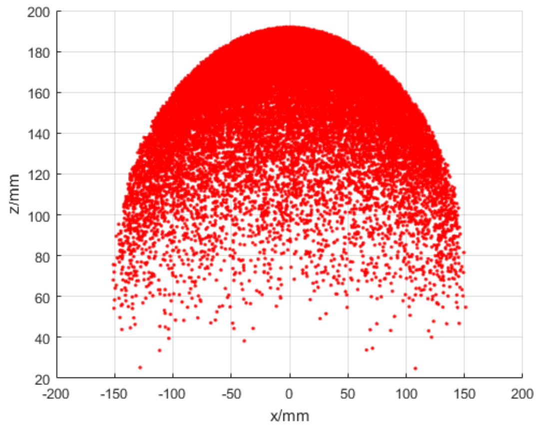

(b)

Fig.4 Workspace of the robot (a) stereo view and (b) *x-z* view

III. PROTOTYPE CONSTRUCTION

A prototype was built as shown in Figure 5. It consists of two parts: continuum robot arm and drive device. Every segment of the robot arm is made of ABS by 3D printing. The drive system consists of a constant speed motor driving a shaft, a microcontroller, a relay module, and six electromagnetic clutches with each connected to one cable. When these electromagnetic clutches are not activated, they are separated from the shaft, so that the cables are not moved by the motor's rotation. If electromagnetic clutches are activated, the cables will be coupled with the motor, so that the robot is controlled accordingly. Since the robot arm has three sections and six DOFs, six clutches were used to control the different bending motion. C_1 and C_6 control the 2 DOFs bending of the first section, C_2 and C_5 for the bending of the second section, C_3 and C_4 the motion of the third section.

IV. NEW CONTROL METHOD: TIME WIDTH MODULATION METHOD

As mentioned in Section 1, a multiple DOFs robot is usually controlled by a number of actuators, and therefore, its control system is complex. This paper proposes a new time-based control method using electromagnetic clutches, in which only one actuator is adopted. As the control method is controlling the cables' displacement based on time via on/off modes of the electromagnetic clutches, similar to the Pulse Width Modulation Method, it is therefore named as Time Width Modulation Method (TWM).

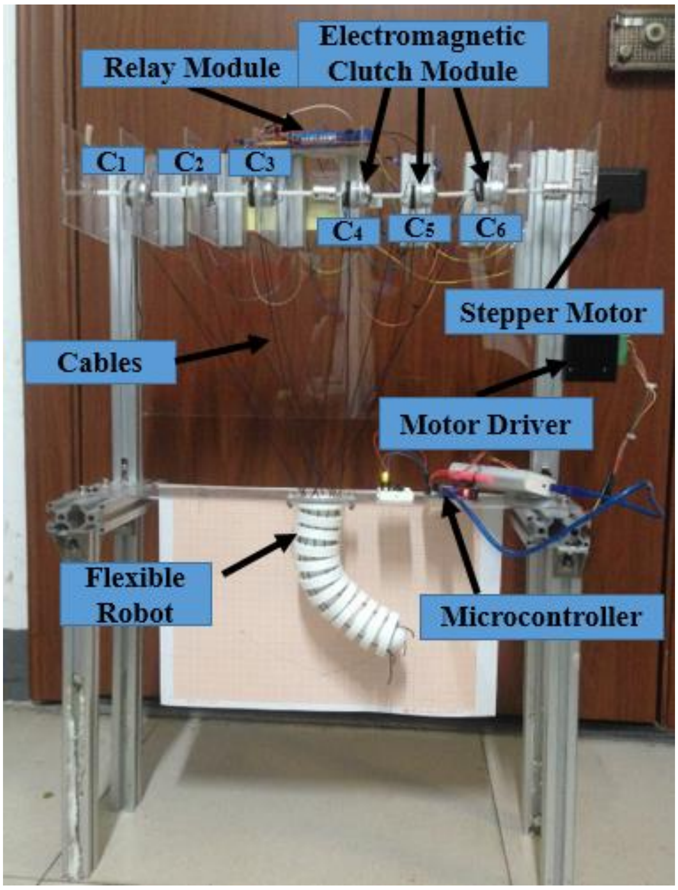

Fig.5 Experimental prototype

A. *displacement - time transformation*

Since the motor is kept at a constant rotational speed, when the clutches are activated, the rotational speed of the cable cylinders is also constant. So the length of the cables can be easily controlled by controlling the activation time of clutches, thereby the motion control of the robot is significantly simplified.

Assuming that the nonlinear properties of electromagnetic clutches is negligible. The rotating speed of motor is *n*, the diameter of the cable cylinder is *d*, and the cable length change *l* can be described as:

$$l = \pi ndt \tag{17}$$

Note that

$$L_1 - L_3 = 2\pi ndt_1 \tag{18}$$

$$L_2 - L_4 = 2\pi ndt_2 \tag{19}$$

So (1) ~ (2) can be described as

$$\Phi = arctan\left(\frac{t_2}{t_1}\right) \quad (20)$$

$$\Theta = N \cdot \theta = 2N \cdot arcsin\left[\frac{\pi n\sqrt{t_1^2 - t_2^2}}{N}\right] \quad (21)$$

By substituting equations (18) and (19) into the kinematics model above, the time-based control can be obtained, and its flowchart is given in Figure 6.

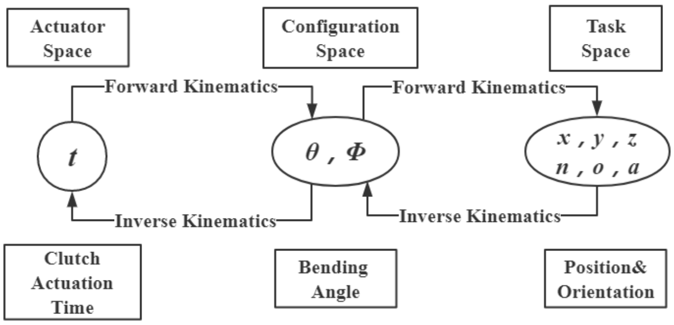

Fig.6 The flowchart of time-based model

B. *time sequence diagram*

To specify the control method, a time sequence diagram, as shown in Fig. 7 is proposed to describe the control process. The diagram illustrates the principle of the control method with different activation time of clutches, the robot can bend in different gestures.

A few specific robot motion cases were demonstrated as shown in Figure 8. The four cases show the different bending gestures of the robot controlled by the four time sequence diagrams as shown in Fig. 9. Each gesture needs specified control instructions. In case (a), only the first section of the robot bends. In cases (b) and (c), the second and third sections of the robot bend separately. In case (d), all the three sections bend together. The four cases show that once the time sequence diagram is determined, the motion and the gesture of the robot are uniquely determined.

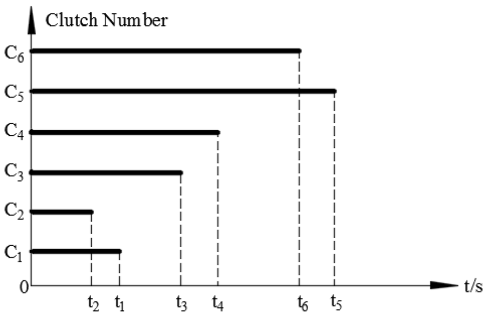

Fig.7 Time sequence diagram

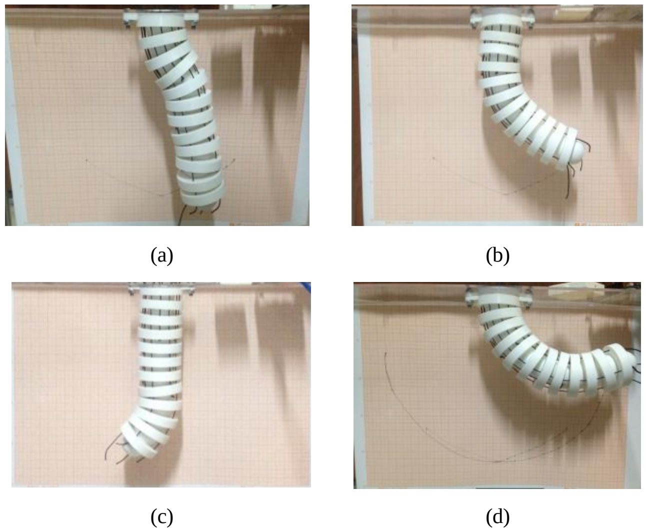

Fig.8 Different bending cases

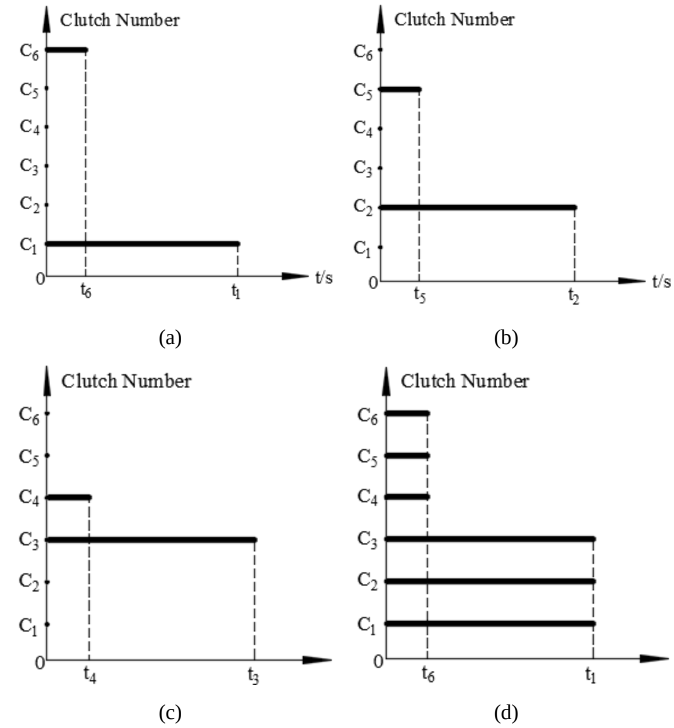

Fig.9 Time sequence diagram of different cases

V. EXPERIMENT

To validate the control method and the design, a series of experiment was carried out. In the experiments, four cases were studied. As shown in Figure 8, different bending angels can control the trajectories of robot. The different bending angles are shown in the Table II.

TABLE II. BENDING ANGLE OF DIFFERENT CASES

Case	**Bending Angle**		
	Section 1	***Section 2***	***Section3***
Case(a)	0~54.72° ($t_1 = 0.9$s $t_6 = 0.6$s)	0	0
Case(b)	0	0~54.72° ($t_2 = 0.9$s $t_5 = 0.6$s)	0
Case(c)	0	0	0~54.72° ($t_3 = 0.9$s $t_4 = 0.6$s)
Case(d)	0~54.72° ($t_1 = 0.9$s $t_6 = 0.6$s)	0~54.72° ($t_2 = 0.9$s $t_5 = 0.6$s)	0~54.72° ($t_3 = 0.9$s $t_4 = 0.6$s)

Figure 10 shows the trajectories of the end effector in the four cases, and the experimental results are compared with the theoretical ones. In the figure, the dots are the recorded trajectories and the solid curves are the predicted trajectories.

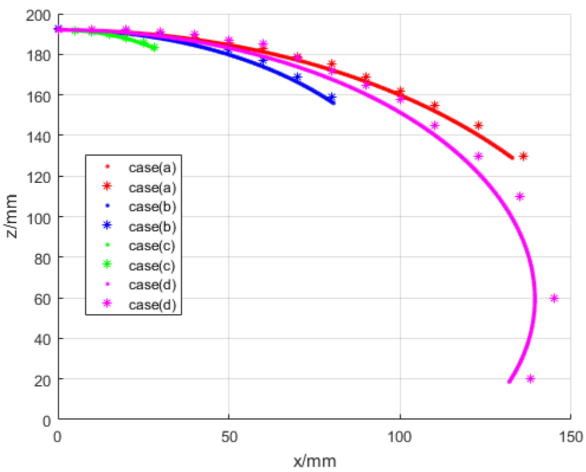

Fig.10 Trajectories of the end effector

As a result, the average relative positioning errors for four cases are: 2.85%、1.48%、1.09% and 5.21%. The data reveals that the control method is valid, and it proves that the error of each section will be accumulated. Additionally, compared with the position error in [11], the error in this paper is acceptable. It also proves that the TWM method for continuum robot is feasible.

VI. CONCLUSION

A new six DOF cable-driven snake-like robot driven by only one motor via six clutches is presented. A new time-based control method named 'time width modulation' is proposed to control the continuum robot. Kinematics model of the robot is developed and its workspace is analyzed. A prototype is built and experimental results demonstrate the effectiveness of the design and the control method. The accuracy of the prototype robot is also obtained as acceptable.

REFERENCES

[1] I. D. Walker, D. Dawson, T. Flash, et al. "Continuum robot arms inspired by cephalopods."*Proceedings of SPIE - The International Society for Optical Engineering*5804(2005).

[2] I. D. Walker "Continuous Backbone "Continuum" Robot Manipulators." *ISRN Robotics* 2013.1.

[3] N. Simaan, "Snake-Like Units Using Flexible Backbones and Actuation Redundancy for Enhanced Miniaturization." IEEE International Conference on Robotics and Automation IEEE, 2006:3012-3017.

[4] M. Rolf and J. Steil, "Constant curvature continuum kinematics as fast approximate model for the bionic handling assistant," *IEEE/RSJ Int. Conf. on Intelligent Robots and Systems*. Vilamoura, Algarve, Portugal, Oct. 2012, pp. 3440-3446

[5] Webster III, J. Robert, A. M. Okamura, N. J. Cowan. "Toward Active Cannulas: Miniature Snake-Like Surgical Robots." *IEEE/RSJ International Conference on Intelligent Robots and Systems* IEEE, 2007:2857-2863.

[6] D.B. Camarillo, et al. "Mechanics Modeling of Tendon-Driven Continuum Manipulators." *IEEE Transactions on Robotics* 24.6(2008):1262-1273.

[7] R. Buckingham, "Snake arm robots." *Industrial Robot* 29.3(2002):242-245.

[8] I.A. Gravagne and I. D.Walker, "Manipulability, force, and compliance analysis for planar continuum manipulators," *IEEE Trans. on Robotics and Automation*, 2002, vol. 18, no. 3, pp. 263-273.

[9] D. G. Choi, B. J. Yi, W. K. Kim. "Design of a spring backbone micro endoscope." *IEEE/RSJ International Conference on Intelligent Robots and Systems* IEEE, 2007:1815-1821.

[10] Z. Li, M.C. Lei, S.M. Yuan. "Design and Analysis of a Biomimetic Wire-Driven Robot Arm." *ASME 2011 International Mechanical Engineering Congress and Exposition* 2011:191-198.

[11] Z. Li, R. Du. "Design and Analysis of a Bio-Inspired Wire-Driven Multi-Section Flexible Robot Regular Paper." *International Journal of Advanced Robotic Systems* 10.10(2013):209-220.

[12] Webster III, J. Robert, B. A. Jones. "Design and Kinematic Modeling of Constant Curvature Continuum Robots: A Review." *International Journal of Robotics Research* 29.13(2010):1661-1683